Available online at www.sciencedirect.com
SCIENCE DIRECT®
Molecular Immunology xxx (2006) xxx–xxx
Molecular Immunology
www.elsevier.com/locate/molimm

Mapping and molecular characterization of novel monoclonal antibodies to conformational epitopes on NH_2 and COOH termini of mammalian tryptophanyl-tRNA synthetase reveal link of the epitopes to aggregation and Alzheimer's disease

Elena L. Paley[a,b,c,*], Larisa Smelyanski[d], Vladimir Malinovskii[c], Pochi R. Subbarayan[c], Yevgeny Berdichevsky[e], Natalia Posternak[e], Jonathan M. Gershoni[d], Olga Sokolova[f], Galina Denisova[d,g]

[a] *Department of Urology, Northwestern University Feinberg School of Medicine, Tarry Research Building 16/759, 303 E. Chicago Avenue, Chicago, IL 60611, USA*
[b] *Expert BioMed, Inc., Miami, FL 33179, USA*
[c] *University of Miami School of Medicine, Miami, FL 33101, USA*
[d] *Department of Cell Research and Immunology, Wise Faculty of Life Sciences, Tel Aviv University, Tel Aviv 69978, Israel*
[e] *Department of Molecular Microbiology & Biotechnology, Wise Faculty of Life Sciences, Tel Aviv University, Tel Aviv 69978, Israel*
[f] *Howard Hughes Medical Institute and Department of Biochemistry, Brandeis University, 415 South Street, Waltham, MA 02454-9110, USA*
[g] *Department of Pathology and Molecular Medicine, Center for Gene Therapeutics, McMaster University, Hamilton, ON, Canada*

Received 24 March 2005; received in revised form 7 February 2006; accepted 9 February 2006

Abstract

Tryptophanyl-tRNA synthetase (TrpRS) is an interferon-induced phosphoprotein with autoantigenic and cytokine activities detected in addition to its canonical function in tRNA aminoacylation. The availability of monoclonal antibodies (mAbs) specific for TrpRS is important for development of tools for TrpRS monitoring. A molecular characterization of two mAbs raised in mice, using purified, enzymatically active bovine TrpRS as the inoculating antigen, is presented in this report. These IgG1 antibodies are specific for bovine, human and rabbit but not *E. coli* TrpRS. Immunoreactivity and specificity of mAbs were verified with purified recombinant hTrpRS expressed in *E. coli* and TrpRS-derived synthetic peptides. One of the mAbs, 9D7 is able to disaggregate fibrils formed by Ser32-Tyr50 TrpRS-peptide. Epitope mapping revealed that disaggregation ability correlates with binding of 9D7 to this peptide in ELISA and immunocytochemistry. This epitope covers a significant part of N-terminal extension that suggested to be proteolytically deleted in vivo from the full-length TrpRS whereas remaining COOH-fragment possesses a cytokine activity. For epitope mapping of mAb 6C10, the affinity selected phage-displayed peptides were used as a database for prediction of conformational discontinuous epitopes within hTrpRS crystal structure. Using computer algorithm, this epitope is attributed to COOH-terminal residues Asp409–Met425. In immunoblotting, the 6C10 mAb reacts preferably with (i) oligomer than monomer, and (ii) bound than free TrpRS forms. The hTrpRS expression was shown to correlate with growth rates of neuroblastoma and pancreatic cancer cells. Immunohistochemically both mAbs revealed extracellular plaque-like aggregates in hippocampus of Alzheimer's disease brain.

Keywords: Monoclonal antibodies; Epitope mapping; Aminoacyl-tRNA synthetases; Aggregation/disaggregation; Neuroblastoma; Pancreatic, cervical and kidney cancer cells; Alzheimer's disease

1. Introduction

Tryptophanyl-tRNA synthetase (TrpRS) is a key enzyme of protein biosynthesis catalyzing $tRNA^{trp}$ aminoacylation. TrpRS belongs to a family of aminoacyl-tRNA synthetases (ARS) existing as free forms and also as components of multi-enzyme com-

Abbreviations: TrpRS, tryptophanyl-tRNA synthetase; mAb, monoclonal antibody; FCS, fetal calf serum; GluRS, glutamyl-tRNA synthetase; ARS, aminoacyl-tRNA synthetases; AD, Alzheimer's disease

* Corresponding author. Tel.: +1 786 390 6028; fax: +1 309 407 9869.
E-mail address: ElenaPaley@cs.com (E.L. Paley).

0161-5890/$ – see front matter © 2006 Elsevier Ltd. All rights reserved.
doi:10.1016/j.molimm.2006.02.006

plex (Norcum, 1989). Although TrpRS was mostly detected as a free cytosolic enzyme, in the earlier report it was also found in association with a multi-enzyme complex (Bandyopadhyay and Deutscher, 1971). Later co-localization of TrpRS with components of the complex such as glutamyl-tRNA synthetase (GluRS) was revealed by immuno-electron microscopy (Ivanova et al., 1993; Popenko et al., 1994). TrpRS consists of two subunits of 54–60 kDa in mammals and of 37 kDa in bacteria (Penneyes and Muench, 1974). TrpRS from different mammalian sources show a high homology. By means of small angle X-ray scattering, an aggregation of beef pancreas TrpRS was observed at physiological and low (4–8 °C) temperatures when electrophoretically homogenous preparation was found to be heterogeneous in particle sizes (Tuzikov et al., 1991). At heating up to 30–45 °C, the oligomer sizes increased as well as its proportion with formation of the aggregates 10 times exceeding the sizes of initial particles. We revealed earlier the large aggregates (up to 0.5 μm) immunoreactive with anti-TrpRS antibodies in the cytoplasm of bovine kidney MDBK cells by immunoelectron microscopy (Paley et al., 1991). The aggregation of the other ARS includes the loss of alpha-helices concomitant with the formation of intermolecular beta-sheets in GluRS (Lefevre et al., 2004). According to the previously reported immunochemical study with polyclonal antibodies, the bovine TrpRS (bTrpRS) has about 10 antigenic determinants non-randomly scattered along the polypeptide chain (Scheinker et al., 1979). The two of three earlier studied monoclonal antibodies (mAbs) against bTrpRS exerted no effect on aminoacylation of $tRNA^{trp}$ whereas one mAb inhibited the enzymatic activity (Beresten et al., 1989). We showed that TrpRS is a phosphoprotein (Paley et al., 1991; Paley, 1997), which role in a tumor progression is suggested (Paley, 1999). TrpRS is the only ARS member, which is highly induced by interferons (Rubin et al., 1991). TrpRS is also up-regulated during monocyte to macrophage maturation (Krause et al., 1996), maturation of immature dendritic cells (Matsunaga et al., 2002), in the developing Drosophila salivary gland (Seshaiah and Andrew, 1999), by erythropoietin in human vascular endothelial cells (Fodinger et al., 2000) and during skin delayed-type hypersensitivity reaction induced by protein antigens (Ohtani et al., 2004). Some ARS are discovered to be human autoantigens. Specifically, the autoantibodies against several ARS are revealed in myopathies (Ramsden et al., 1989; Miller et al., 1990; Targoff, 2002). The TrpRS-directed autoantibodies are also present in autoimmune diseases (Vartanian, 1991; Bolgarin et al., 1998) and apparently non-autoimmune conditions (Paley et al., 1995). TrpRS possesses activity of an interferon-induced inflammatory cytokine (Salvucci et al., 2004). In spite of the potential medical significance it has not been studied yet immunohistochemically under different physiological and pathological conditions and no mAbs directed to the native mammalian TrpRS are currently available. The availability of such antibodies is of a vital importance since the intensive inflammatory reactions can lead to the tissue damage, when toxic levels of inflammatory cytokines are produced. To develop tools for TrpRS detection under different conditions including those presumably associated with the interferon induction and inflammation, the novel mAbs against the native bTrpRS were generated in mice and characterized with particular reference to the mapping of the antigenic epitopes and examination of mAb activities. The immunoreactivity of mAbs was explored with the new-constructed recombinant human TrpRS (hTrpRS) and TrpRS-derived synthetic peptides. The combinatorial phage-display peptide library together with a computer algorithm for prediction of discontinuous epitopes (Enshell-Seijffers et al., 2003) was employed for identification of TrpRS epitope within a crystal structure of hTrpRS (Yang et al., 2003). The presence of TrpRS epitopes was analyzed immunocytochemically and immunohistochemically.

2. Materials and methods

2.1. Monoclonal antibodies to TrpRS

A single immunization of purified native enzymatically active bTrpRS, a Fractogel fraction (Paley, 1997) in complete Freund Adjuvant was given to mice Balb/c and was followed by the 20, 40 and 30 μg peritoneal injections of bTrpRS in non-complete Freund Adjuvant with the intervals 3 weeks. The 3 weeks after the last injection, one of the mice was boosted into the tail vein with TrpRS (50 μg) in PBS. After 3 days the splenocytes were isolated, fused with NSO myeloma cells and seeded on ten 96-well plates by standard procedure (Galfre and Milstein, 1981). The 21 positive clones were selected after ELISA screening with the purified bTrpRS (5 μg/ml) as a coating antigen. The two clones 6C10 (mAb B1) and 9D7 (mAb B2) were recloned and examined as hybridoma supernatants. The mAbs were purified from supernatants containing 20% FCS by sequential precipitation with caprylic acid and $(NH_4)_2SO_4$ (Harlow and Lane, 1988) and lyophilized or purified from ascites fluids generated in mice. The mAbs purity was estimated >70% in SDS-PAGE and isotype was determined using commercial kit (Roche Diagnostics GmbH, Isostrip, mouse mAb isotyping kit).

2.2. Recombinant hTrpRS

The hTrpRS gene (Frolova et al., 1991) was amplified by PCR from a human fetal kidney cDNA λgt10 phage library (Clontech) with TaKaRa Ex Taq™ polymerase applying primers 5′-ATGCCCAACAGTGAGCCCGCATCTCTG-3′ and 5′-CTACTGA-AAGTCGAAGGACAGCTTCCG-3′ for termini N and C, respectively. Following the TrpRS gene DNA sequencing the *Nde*I restriction site was introduced on both termini by a second PCR using the *Nde*I restriction site-tagging primers 5′-ACAGACCGACATATGCCCAACAGTGAGCCCGCA-3′ for the N-terminus and 5′-ACAACGTATCATATGCTACTGAAA-GTCGAAGGACAG-3′ for the C-terminus. The 1443 base pair (bp) PCR product was digested with *Nde*I and cloned into plasmids pET11c and pET14b (Novagen). *E. coli* XL-1 Blue cells (Stratagene) were used for plasmid DNA propagation. Plasmids pET11c and pET14b containing hTrpRS gene in the correct orientation confirmed by *Bam*HI analysis were used to transform *E. coli* strains BL-21 (DE3, pLysS) (Novagen). The cell extracts of the plasmid pET11c containing an intact hTrpRS and plasmid pET14b containing hTrpRS fused to His_6-Tag followed by

a thrombin site at the N-terminus, were analyzed by SDS-PAGE and Western blot. The well-characterized polyclonal antibodies to bTrpRS (Paley et al., 1991; Paley, 1999) and purified bTrpRS (Paley, 1997) were used as standards. The His_6-Tagged hTrpRS was purified from the soluble fraction on a Qiagen Ni-NTA agarose column as described (Du and Novick, 2001).

2.3. Immunocytochemsitry by mAbs blocked with recombinant hTrpRS

Human pancreatic MIA PaCa-2 (1420) (Yunis et al., 1977), Panc-1 (1469) (Lieber et al., 1975) and cervical HeLa cancer cells were from American Type Culture Collection. The cells were grown in DMEM with high glucose/10% FCS/14 μg/ml gentamycin (all Gibco) at 37 °C/5% CO_2. For immunocytochemistry the semi-confluent cells grown in 6, 12 (Falcon) or 24-wells (Corning) plates were treated with ice cold 80% methanol for 30 min or 4% formaldehyde/PBS for 10 min, 0.5% Triton X-100/PBS for 5 min and then blocked with 1% gelatin/PBS for 90 min at room temperature or with 10% FCS/0.1% NaN_3/PBS for 30 min or overnight at 4 °C. The cells were incubated with mAbs to TrpRS and then with peroxidase/anti-mouse antibodies (Jackson ImmnunoResearch or Amersham) at 1:500 for 30 min/room temperature. The cells were washed with PBS following incubations, developed with AEC kit (Sigma), counterstained with Mayer's hematoxylin (Sigma) or analyzed without counterstaining by light microscopy (Olympus and Nikon). The controls omitted anti-TrpRS antibodies were treated with the only secondary antibodies. For depletion, the TrpRS-antibody was preincubated with bovine serum albumin (BSA, Sigma) or ~8-fold molar excess of hTrpRS purified from the soluble fraction of DH5α cells (Invitrogen) bearing pET14b $hTrpRS^+$.

2.4. Real-time RT-PCR analysis of TrpRS gene expression in human pancreatic cells

Total RNA from MIA PaCa-2 and Panc-1 cells were prepared using Tri-Reagent (Sigma). The oligonucleotides used for β-Actin are: 5′-TCACCCACACTGTGCCCATCTACGA-3′ (F) and 5′-CAGCGGAACCGCTCATTGCCAATGG-3′ (R) and for hTrpRS are: 5′-GCACTGCTTGTCTGTACTGTCCAT-3′ (F) and 5′-ATCTCTGCTGGAGCTGTTCAAC-3′ (R) (Miami University DNA facility). For the first cDNA strand synthesis, RNA (2 μg) was transcribed using M-MLV reverse transcriptase as recommended (Promega). The first strand mixture (5 μl) was used for the second strand synthesis. The real-time RT-PCR was performed on GeneAmp Sequence Detection System 5700 (Applied Biosystem) with β-Actin gene as an internal reference. The mean normalized expression was calculated (Muller et al., 2002).

2.5. Screening of phage display library and sequence of selected peptides

Biopanning of phage display epitope library, immunoscreening, dot blot and sequencing were performed as described (Enshell-Seijffers et al., 2001; Enshell-Siejffers and Gershoni, 2002).

2.6. Computer algorithm

Prediction of epitopes was performed by D.A. Denisov's method. The amino acid sequences of the selected phages were used as a database for computer algorithm (Enshell-Seijffers et al., 2003).

2.7. Introduction of 6C10 epitope into vector fth1

The bacteriophage vector fth1 was digested with *Sfi*I enzyme (Enshell-Seijffers et al., 2001, 2003). The purified linear vector was ligated with 6C10 epitope encoding linker produced by annealing the two complementary oligonucleotides 5′-tgatgatgataaactggaacagattcgtcgtgattataccagcggggcagcgtctg-3′ (56 bases) and 5′-acgctgccccgctggtataatcacgacgaatctgttccagtttatcatcatcacgt-3′ (56 bases). The vector was transformed into DH5α *E. coli* cells. The selected phages with and without 6C10 epitope were prepared for immunodot-blot and DNA analyses.

2.8. Dot-blot analysis of 6C10 epitope presenting phages

The phages (10^{10} to 10^{11}/50 μl/well) were applied via a vacuum manifold to a nitrocellulose membrane. After blocking with 5% milk/Tris-buffered saline (TBS) for 1 h, the membrane was washed with TBS and incubated with an undiluted 6C10 hybridoma supernatant for 75 min at room temperature in TBS/5% milk. After washing, the membrane was incubated with peroxidase goat anti-mouse IgG (1:2500) in TBS/5% milk for 1 h at room temperature and developed with ECL (Amersham). The clones were examined in duplicates. The purified bTrpRS was used as a positive control. The self-ligated vector without 6C10 and non-ligated vector fth1 were applied as controls.

2.9. Peptide synthesis, purification and characterization

TrpRS-derived peptides were synthesized on a single substituted Fmoc amino acid Wang resin in the presence of HOBt and diisopropylcarbodiimide in DMF. Fmoc derivatives of L-amino acids and Model 350 Multiple Peptide Synthesizer were from Advanced Chemtech. Nascent polypeptide chains were cleaved by Reagent K (TFA–phenol–thioanisol–ethanedithiol–water, 82.5:5:5:2.5:5), extracted by ether, dried, resuspended in acetonitrile, and lyophilized. Mass spectra were recorded on MALDI-TOF Kompact SEQ mass spectrometer (Kratos Analytical-Shimadzu). The TrpRS-peptides were identified as positively charged single parent ions ($M+H+$) with purity >90%. All peptides were hydrophilic.

2.10. ELISA of TrpRS-synthetic peptides with mAbs against TrpRS

Fresh aqueous solutions of lyophilized synthetic peptides (1, 1.3, 2, 2.5 and 5 mg/ml in 50–100 μl) were loaded onto vir-

gin polysterene plates (Nunc, immuno maxisorp) for 20 h at room temperature. The plates were incubated with 1% gelatin (Sigma)/PBS (100 μl, blocking solution) for 1–2 h, with mAbs (0.15–20 μg/50–100 μl blocking solution) for 1, 2.5, 2.75 and 20 h and then with peroxidase goat antibodies to mouse IgG (Jackson Immuno Research) at 1:2500 (N, M and C peptides) and 1:3700; 1:5000; 1:10,000 and 1:15,000 (N-peptide) for 1 h at 37 °C. Reaction was developed with 1, 1.3 (20-h mAb incubation) or 2 mg/ml 2,2′-azino-bis (3-ethylbenz-thiazoline-6-sulfonic acid) diammonium salt (ABTS) in 50 mM Na_2HPO_4, 24 mM citric acid with 0.08%, 0.1% (20 h) or 0.15% H_2O_2 (Sigma). The samples were tested in duplicates, triplicates or quadruplicates. The anti-TpRS antibodies or peptides or both peptides and anti-TrpRS antibodies were omitted in the blanks. Plates were washed four times with PBS between incubations and monitored at 405 nm in the Microplate reader Benchmark Plus (Bio-Rad).

2.11. Blocking of immunocytochemical reaction with TrpRS-derived synthetic peptides

Immunocytochemistry of human cells was performed as described above. The anti-TrpRS mAbs were depleted with a molar excess of TrpRS synthetic peptides.

2.12. Congo red staining and birefringence of peptides

The amyloid fibrils are characterized by green birefringence in Congo red. The water solutions of each peptide (1–10 mg/ml) were stored at room temperature for 1 or 18 h. The purified recombinant hTrpRS (8 mg/ml) from a soluble fraction of DH5α *E. coli* cells was stored at 4 °C in the buffer described above with diisopropylfluorophosphate. A drops (2 μl) of each peptide or hTrpRS were placed on the glass slides, air-dried and stained with 1% Congo red/1% NaOH/80% ethanol (v/v) for 5 min. The slides were examined in the microscope bright field and polarized light.

2.13. Electron microscopy of the peptides

The freshly prepared water solutions of synthetic peptides (≤5 mg/ml) were immediately applied onto the carbon-coated glow-discharged copper 400 mesh grids. Grids were negatively contrasted with 1% uranyl acetate and washed twice with water. Grids were examined in a Philips CM-12 electron microscope at 120 kV at 60 K magnification and −1.5 μm under focus low-dose conditions. The negatives were digitized in a Zeiss SCAI scanner using the 7 Å/pixel compression as described (Sokolova et al., 2003).

2.14. Effect of peptides on human cells growth

The aqueous solutions of peptides (1 mg/ml) were added to the medium at the different final concentrations in triplicates. The (4–6) × 10^4 cells/well of MIA PaCa-2 (1420) and Panc-1 (1469) were seeded on 24-wells plates in DMEM with high glucose/10% FCS. The incubation with peptides was for 24 and 48 h. The cells were counted in a hemacytometer based on trypan blue exclusion.

2.15. Preparation of mammalian cell extracts

The rabbit kidney LCC-RK1 cells (Hull et al., 1965) from American Type Culture Collection and human neuroblastoma SH-SY5Y cells (Biedler et al., 1973) from Weizmann Institute (Israel) were cultivated in RPMI 1640 or DMEM, 10% FCS and antibiotics. The cells washed twice with PBS were collected by scraper and extracted by quick freezing/thawing in 50 mM Hepes, pH 7.4; 50 mM KCl; 2 mM $MgCl_2$ and a tablet of protease inhibitors cocktail (Roche Mol. Biochem.) per 3–5 ml. The extracts were spun at 8500 rpm in mini centrifuge at 0 °C and supernatants were used for gel filtration or immunoprecipitation.

2.16. Gel filtration of human cell extract

The SH-SY5Y extract (∼1 mg/170 μl) was applied on a 0.7 cm × 50 cm Sephacryl S400 column equilibrated with 50 mM Hepes, pH 7.4, 0.1 M KCl, 2 mM $MgCl_2$ and 1 tablet/5 ml of protease inhibitors cocktail (Boehringer). The 0.75 ml fractions were eluted with the same buffer. The TrpRS and GluRS aminoacylation activities were measured in 40 fractions by adding aliquots (70 μl) to the aminoacylation mixture (30 μl). The Dextran Blue (2 × 10^3 kDa), catalase (250 kDa) and BSA were used for the column calibration. The catalase enzymatic activity was measured in fractions. The protein concentration was determined by Bradford.

2.17. Aminoacylation of tRNA

The aminoacylation mixture (100 μl) contained 0.5 μCi of [^{3}H] tryptophan (33 Ci/mmol, Amersham), or [^{3}H] glutamic acid (44 Ci/mmol, NEN), 250 mM Tris–HCl, pH 7.5, 5 mM ATP, 5 mM $MgCl_2$, 0.2 mM EDTA and 0.2 mg/ml BSA. The activity was measured with 0.1, 10, 50, 100 and 500 μM tryptophan and glutamic acid, the 6, 10 or 17 μg/probe of cell total proteins and 200 μg/probe of rabbit liver total tRNA. Incubations were for 10, 15, 20, 30 and 35 min at 37 °C. For control all compounds were mixed at 0 °C and terminated immediately by 10% trichloroacetic acid.

2.18. Immunoprecipitation

The SH-SY5Y (∼200 μg) or LCC-RK1 (∼40 μg) cell proteins (100 μl) were incubated overnight at 4 °C with anti-TrpRS hybridoma undiluted supernatants (200 μl) or anti-GluRS mAb F25 ascites fluid (1.5 μl) (Filonenko et al., 1991) and then with protein G agarose (110–150 μl) pre-washed in 0.5% NP 40/1 M NaCl (NET). The immunoprecipitates were washed three times with ice-cold NET, pH 7.2 containing 1 M NaCl, 2 M NaCl and 0.1 M NaCl, eluted with SDS-Laemmli buffer at 95 °C for 5 min and separated by 10–12% SDS-PAGE.

2.19. Triton extraction

The epithelial-like fraction of SH-SY5Y cells were lysed in 0.1 M Hepes buffer, pH 6.9, 0.5% Triton X-100, 1 mM $MgCl_2$, 0.1 mM EDTA, 2 mM EGTA, 1 mM DTT, 1 mM PMSF, 0.4 mg/ml aprotinin, 0.1 mg/ml antipain, leupeptin, pepstatin, and hemastatin, 0.1 μM okadaic acid, 10 mM sodium ortovanadate, and 50 mM sodium fluoride in situ (1 ml of buffer/8 cm plate) for 20 min at room temperature. Detergent-insoluble fraction was collected with scraper, washed in the same buffer excluding inhibitors of phosphatases, solubilized in SDS-sample buffer at 100 °C for 5 min and spun.

2.20. Immunoblotting

After SDS-PAGE proteins were transferred onto nitrocellulose or PVDF membranes and blocked with 5% dry milk/PBS. Blots were probed with 6C10 hybridoma supernatant (1:5), 9D7 undiluted supernatant, rabbit polyclonal anti-TrpRS antibodies (1:100) or anti-GluRS mAb F25 for 1 h, washed with PBS/0.1% Tween 20, treated with anti-mouse or anti-rabbit peroxidase-antibodies (Jackson Immuno Research) and developed with ECL or TMB (KPL) reagents.

2.21. Imunohistochemistry of brain sections

The unstained histological slides (Snowcoat^{TM}) with 6-μm thick autopsy brain sections of eight patients with a neuropathologically confirmed Alzheimer's disease were obtained from the Brain Bank of the Mount Sinai Medical Center, NY, USA and provided by Dr. Purohit, D.P., M.D. The brain sections from five non-demented patients were provided by the Israel and Ukrainian Medical Centers. The tissues were fixed for 2 weeks in paraformaldehyde. The paraffin-embedded sections were deparaffinized in xylene, hydrated, incubated with 3% hydrogen peroxide/methanol for 30 min at room temperature and washed in PBS. Then sections were incubated with 0.1–0.3% Triton X-100 for 10–20 min, washed, incubated with 1% BSA for 30 min and then with mAbs to TrpRS overnight at 4 °C. Then sections were incubated with peroxidase-conjugated antibodies for 1 h at 37 °C and developed with 3,3′-diaminobenzidine. The control sections were overlaid with the only secondary antibodies or mAbs blocked with purified recombinant hTrpRS. Sections were counterstained with Highmann's Congo red for 10 min and Harris's hematoxylin for 2 min, mounted and examined under phase-contrast and polarized light or confocal scanning laser microscopy.

3. Results and discussion

3.1. Immunoreactivity of mAbs B1 and B2 with bTrpRS and hTrpRS

We characterize here two mouse mAbs 6C10 (B1) and 9D7 (B2) to purified enzymatically active pancreas bTrpRS. Both clones are immunoreactive with bTrpRS in ELISA and immunodot in native conditions and do not inhibit the $tRNA^{trp}$ aminoacylation (data not shown). The subtype determined for both mAbs is IgG1. The clones are characterized further by immunoblotting with bTrpRS used for immunization (Fig. 1) and also with recombinant hTrpRS expressed in *E. coli* (Figs. 1 and 2). In Western immunoblotting under reducing

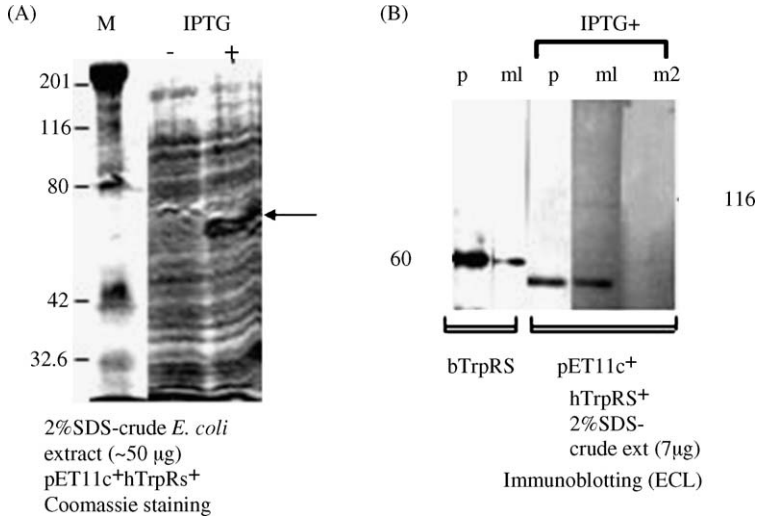

Fig. 1. Western immunoblotting of purified bTrpRS and recombinant hTrpRS with anti-TrpRS antibodies. (A) Recombinant hTrpRS expressed in AD 494 (DE-3) *E. coli* cells bearing plasmid pET11c (hTrpRS$^+$ without His_6-Tag). The cells were grown in LB with 100 μg/ml ampicilin and 100 μg/ml kanamycin overnight. Then cells were grown in TB medium containing 100 μg/ml ampicilin for 3 h until OD_{600} = 0.4 OE. The portion of these cells was extracted with the buffer containing 2% SDS, 100 mM dithiothreitol, 50 mM Tris HCl, pH 6.8 and used as an uninduced control. Then cells were incubated with 1 mM IPTG for 2.5 h at 37 °C and extracted as the control cells. The cell pellet of 1 ml of the bacterial culture was extracted with 100 μl of the 2% SDS-buffer and stored at −20 °C. The extracts were thawed and heated at 70 °C, for 5 min. The samples (25 μl) were loaded on SDS-12% PAGE (~50 μg of the crude *E. coli* extract/lane), Kaleiodoscope prestained standards (Bio-Rad) were run on the same gel (M). The gel was stained with Coomassie blue. Note ~5 μg of ~55 kDa polypeptide (arrow) out of ~50 μg of the crude SDS-cell extract was induced by IPTG. (B) Western immunoblotting of bTrpRS (0.5 μg) and 3.5 μl of preboiled crude SDS extract/well (~5–7 μg/well) with polyclonal Ab to bTrpRS (p), mAb B1 (m1) and mAb B2 (m2). Note ~0.5–0.7 μg of recombinant hTrpRS is detected with a mAb B1 (6C10) hybridoma supernatant (ECL).

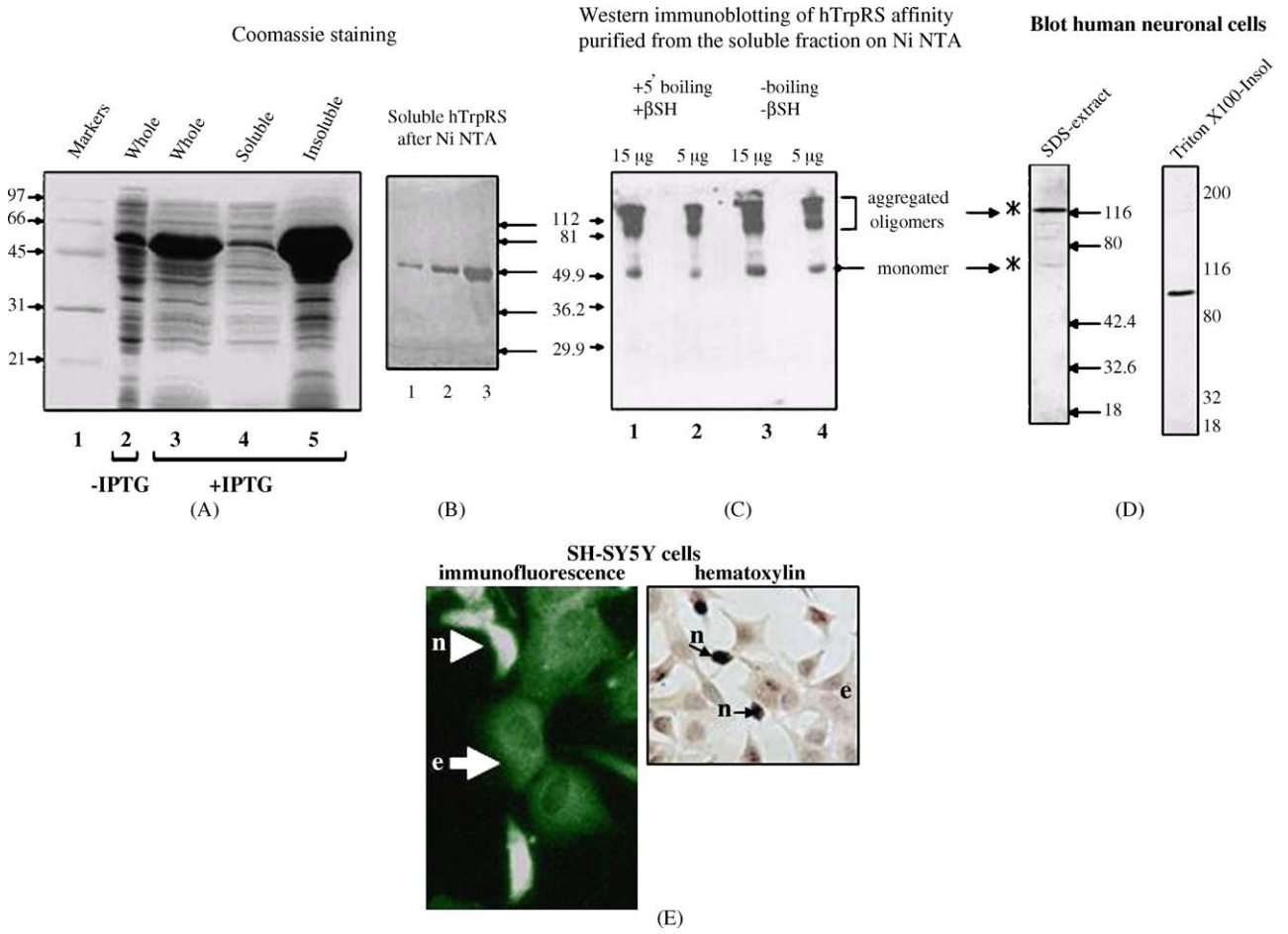

Fig. 2. Detection of hTrpRS oligomer form with 6C10 (mAb B1). (A) Coomassie staining of SDS-PAGE of the *E. coli* cell extracts before (lane 2) and after induction with IPTG (lanes 3–5). Lane 4 shows a soluble fraction and lane 5 is an insoluble fraction after the IPTG induction. Lane 1 includes the molecular weight markers. The fractions were extracted from BL21 (DE-3, PlysS) *E. coli* cells bearing plasmid pET14b hTrpRS^{+}. (B) Coomassie staining of SDS-12.5% PAGE of hTrpRS purified from the soluble fraction on the Ni NTA column. Lane 1 shows fraction eluted with the buffer containing 100 mM imidazole, the lanes 2 and 3 are fractions eluted with 150 mM imidazole. The samples were preboiled in the presence of β-mercaptoethanol before PAGE. (C) Immunoblotting of the His_6-hTrpRS purified on Ni NTA column. Lanes 1 and 3: 15 μg of the protein/well; lanes 2 and 4: 5 μg of protein/well. Lanes 1 and 2, the samples after preboiling (5 min) with 4% β-mercaptoethanol (β-SH), lanes 3 and 4, without boiling and β-SH. The recombinant hTrpRS linked to His_6-Tag at the N-terminus was isolated from the soluble fraction (Du and Novick, 2001). The blot was incubated with the undiluted supernatant of mAb B1. (D) Western blotting and (E) immunofluorescence (left panel) of the epithelial-like cell fraction of SH-SY5Y cells with mAb 6C10 undiluted hybridoma supernatant. The different adhesive abilities of neuroblasts (n) and epithelial-like cells (e) were employed for the cell selection (the right panel in E shows hematoxylin staining). To enrich culture with epithelial-like cells, the neuroblasts were washed out during passages of the old SH-SY5Y culture. (D) Western blotting was conducted with ~80 μg of pre-boiled total 2% SDS/4% β-mercaptoethanol-extract (10%/12% PAGE) and 0.5% Triton X-100-insoluble extract (8%/12% PAGE) of the epithelial-like enriched SH-SY5Y cells (peroxidase-secondary antibody, ECL). Immunoblot with extracts of SH-SY5Y cells containing majority of neuroblasts (>97%) showed no ECL signal. For immunofluorescence (E, left) the SH-SY5Y cells were fixed with 4% formaldehyde (Merck), 0.25% glutaraldehyde (Sigma)/PBS for 30 min, pretreated with 1% Triton X-100/PBS for 10 min and then incubated with mAb 6C10 overnight at 4 °C. The incubation with the secondary FITC anti-mouse goat IgG antibody (1:32; 1 mg/ml, Sigma) was for 1 h at room temperature. The negative controls for immunofluorescence and Western blotting included incubation with non-secretory hybridoma supernatant, secondary antibodies and 6C10 mAb blocked with recombinant hTrpRS.

conditions the mAb 6C10 recognized the bTrpRS of ~60 kDa whereas mAb 9D7 shows no reactivity (Fig. 1B). To test the specificity of immunoreactivity we have selected vector pET11c containing plane hTrpRS and vector pET14b bearing hTrpRS linked to His_6-Tag on its amino terminus. The polypeptide of ~55 kDa was highly expressed in the *E. coli* strains bearing both pET11c (Fig. 1A) and pET14b (Fig. 2) plasmids. The single polypeptide of ~55 kDa was recognized in 2% SDS-crude extract of *E. coli* cells bearing pET11c by the well-characterized rabbit polyclonal Ab to bTrpRS (Paley et al., 1991; Paley, 1999) and mAb 6C10 but not mAb 9D7 (Fig. 1B). The mAb 6C10 detected ~0.5–0.7 μg of protein by immunoblotting of the *E. coli* crude extract$^{hTrpRS^{+}}$ developing one ECL signal of a low to moderate intensity (Fig. 1B). Note no crossreactivity of the mAbs with *E. coli* TrpRS 37 kDa polypeptide was detected by immunoblotting. In *E. coli* cells bearing plasmid pET14b$^{hTrpRS^{+}}$ the polypeptide of hTrpRS (~55 kDa) is highly induced by IPTG preferably in the insoluble fraction (Fig. 2A). The hTrpRS was affinity purified from the soluble fraction (Fig. 2B) and examined by immunoblotting with 6C10 mAb (Fig. 2C). The Coomassie staining of the SDS-PAGE visualizes a single polypeptide of ~55 kDa (Fig. 2B) whereas two forms were detected by West-

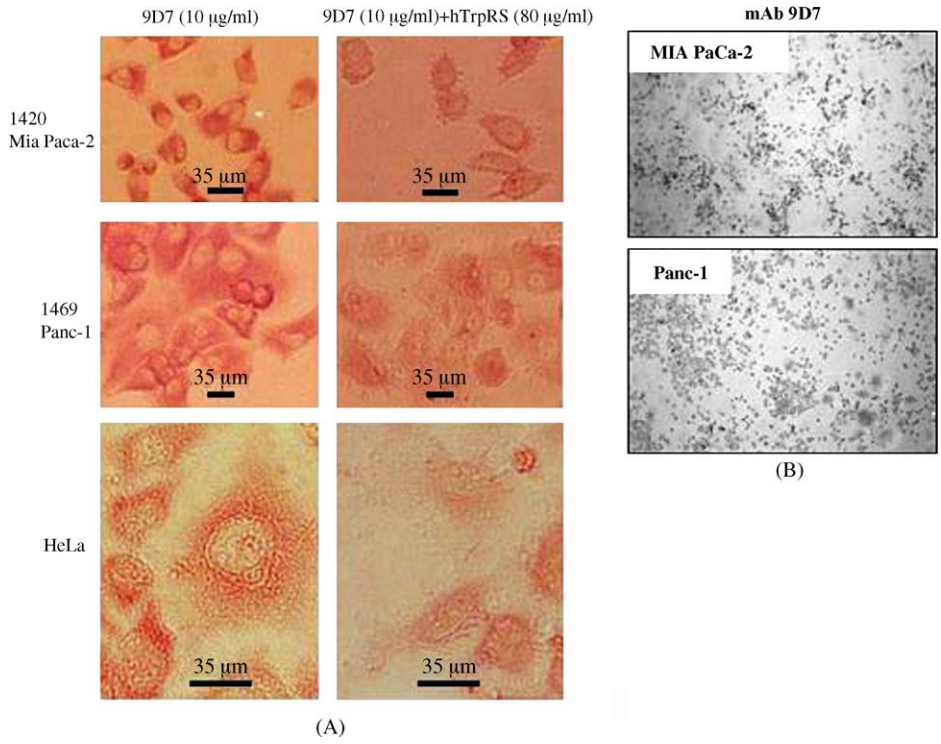

Fig. 3. Differential expression of TrpRS in human cancer cells detected by mAb 9D7 (mAb B2). (A) Blocking of the human cells immunostaining (methanol fixation) with a molar excess of recombinant hTrpRS purified from the soluble fraction of DH5α *E coli* cells on Ni NTA agarose following by the ammonium sulfate extraction (45–55%) and gel filtration on Superdex 200HR. The 1420, 1469 and HeLa cells and were grown on 24-wells plate. The cells were fixed with the ice-cold 80% methanol (0.5 ml/well) for 30 min and incubated with 0.5% Triton for 5 min. Then cells were incubated with 1% gelatin, 10% FCS, 0.1% NaN_3/PBS, pH 7.2 overnight at 4 °C. Cells were incubated with 10 μg/ml of purified mAb B2 (initial concentration 10 mg/ml, dilution 1:1000)/1 mg/ml BSA, 0.02% NaN_3/PBS, pH 7.2 overnight at 4 °C. For depletion of antibody 9D7 the 25 μg/2.5 μl (10 mg/ml) of mAb B2 were added to 200 μg/25 μl (8 mg/ml) of purified soluble hTrpRS in 2.5 ml of buffer as above (the final concentrations were 10 μg/ml of mAb were and 80 μg/ml of hTrpRS) and incubated overnight at 4 °C. The mAb B2 with and without hTrpRS were spun in Beckman mini centrifuge at 12,000 rpm, 4 °C, for 15 min and then incubated with cells overnight at 4 °C. Cell were washed four times with PBS for 30 min, incubated with peroxidase anti-mouse IgG antibodies (Amersham) at 1:400 for 30 min at room temperature and developed with AEC kit. The right panels visualize immunocytochemistry after blocking with the recombinant hTrpRS. Note the control samples on the left panels show immunocytochemistry of the cells with mAb B2 preincubated with 1 mg/ml BSA. The amino terminal sequence of purified hTrpRS confirmed the presence of SSG linker and a six-histidine tag. The sequencing hTrpRS DNA from pET14b revealed a single mutation of Asp37 to Val. Bars = 35 μm. (B) Immunostaining of MIA PaCa-2 and Panc-1 (4% formaldehyde/PBS) with purified mAb B2 (6 μg/ml) as described above (small magnification).

ern immunoblotting of this protein: the monomeric of ∼55 kDa and oligomeric of ≥100 kDa with a preference for oligomers (Fig. 2C). The decrease in immunoreactivity of both forms was observed after boiling in the presence of β-mercaptoethanol. In earlier studies the oxidation and alkylation of Cys-residues led to dissociation of two-subunits of bTrpRS with formation of enzymatically inactive single subunit (Gros et al., 1972; Iborra et al., 1975) and inactivation of hTrpRS (Lipscomb et al., 1976). In Western blotting of the SDS-extract and Triton X-100-insoluble fraction of the epithelial-like enriched fraction of SH-SY5Y cells, a predominant oligomeric forms of ≥100 kDa were revealed by mAb 6C10 (Fig. 2D) whereas no imunoreactivity was detected in the extract of SH-SY5Y neuroblasts (data not shown). The Triton X-100-insoluble cell fractions normally include cytoskeleton and aggregated proteins. It should be noted that SH-SY5Y cells contain ≥97% of the fast-dividing neuroblasts and less than 3% of the slow-dividing epithelial-like cells (Biedler et al., 1973). In contrast to immunoblot, the immunofluorescence of SH-SY5Y cells with mAb 6C10 visualizes apparently stronger immunoreactivity in neuroblasts than in epithelial-like cells (Fig. 2E).

Similarly the MIA PaCa-2 cells express higher level of TrpRS than the slower-growing Panc-1 as detected immunocytochemically with mAb 9D7 (Fig. 3A and B). This data are supported by quantitative real-time RT-PCR analysis, which showed that hTrpRS gene expression is 13 times higher in MIA PaCa-2 than in Panc-1 cells (data not shown). To examine the specificity of immunocytochemistry, the mAb B2 was depleted with a molar excess of the purified recombinant hTrpRS. The cytoplasmic immunostaining of MIA PaCa-2, Panc-1 and HeLa cells with mAb B2 was blocked by recombinant hTrpRS (Fig. 3A). These data indicate that mAb B2 specifically recognize TrpRS in human cells (Fig. 3B).

3.2. Mapping of mAb B2 (9D7) epitope with synthetic TrpRS-derived peptides

Both mAbs were probed with few synthetic peptides (Fig. 4A and B) derived from amino (N), carboxyl (C) and middle (M) parts of hTrpRS. The mAb B2 was found to have affinity to hTrpRS peptide 32-50 (N) located close to the N-terminus. The N-peptide strongly reacted with this antibody in ELISA

(A)

TrpRS-peptides	Amino acid sequence	Position
N	SKDEIDSAVKMLVSLKEMSY	32-50
M	PRIGYPKPALLHSTFFPALQGAQT	329-348
C	EQIRKDYTSGAMLTGELKKALIEV	414-437

(B)

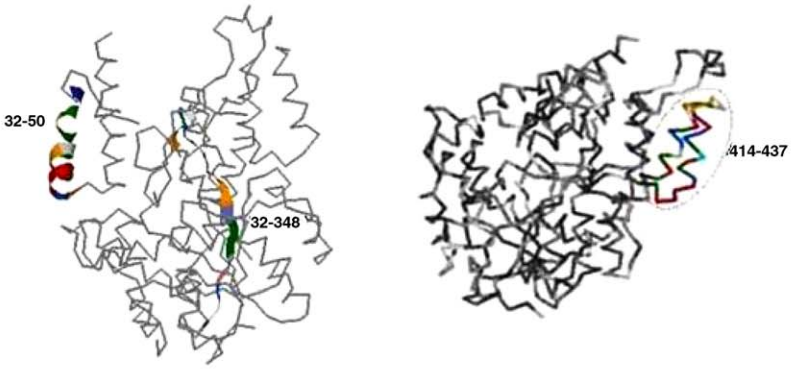

(C)

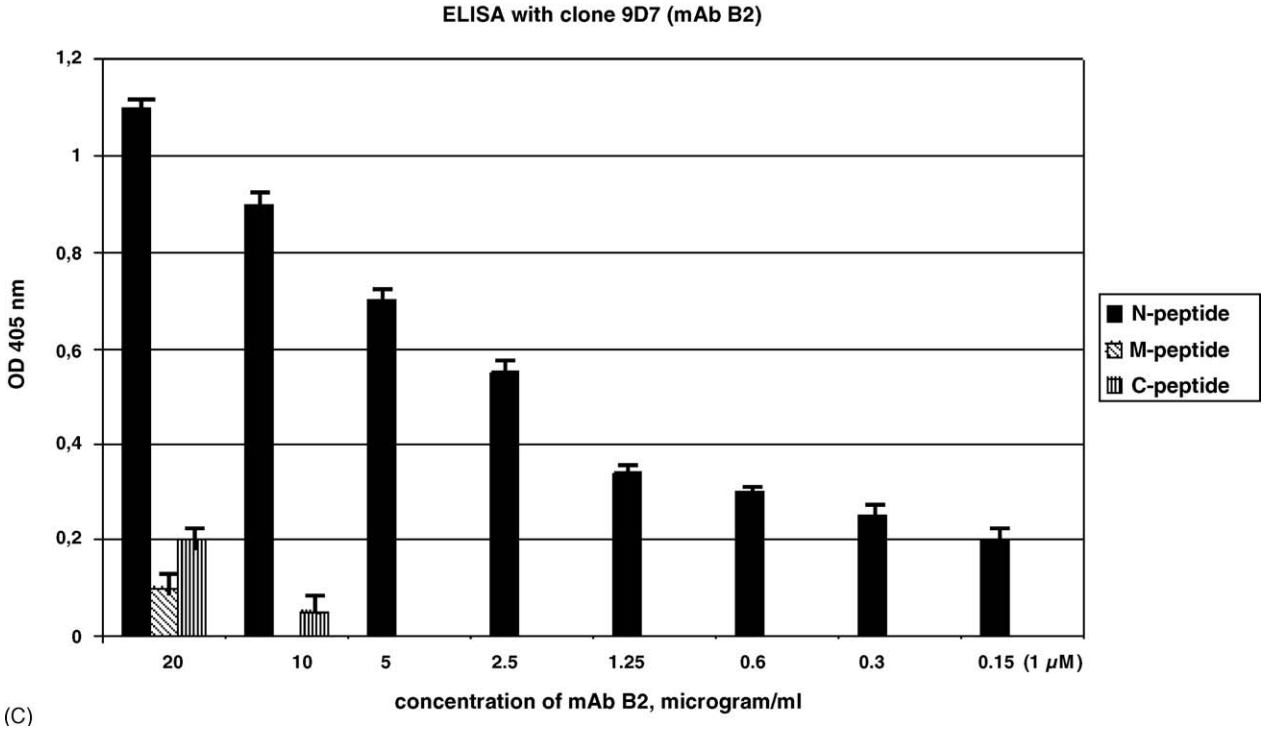

Fig. 4. Epitope mapping of mAb B2 with TrpRS-derived synthetic peptides by ELISA. (A) The TrpRS synthetic peptides. (B) The synthetic peptides within the hTrpRS three-dimensional structure (Yang et al., 2003) are shown as a ribbon presentation. (C) ELISA of the TrpRS-synthetic peptides with mAb B2. The peptides at the concentration 1.3 mg/ml (540 μM) were immobilized on plates overnight at room temperature. The mAb B2 at the concentrations 1–133 μM were added for 20 h.

(Fig. 4C) and also competed with the cellular TrpPS for binding to mAb B2 in immunocytochemistry of 1420, 1469 and HeLa human cells fixed with a methanol (Fig. 5A) or formaldehyde (Fig. 5B). In contrast, the peptides M and C are not strongly reactive with mAb B2 in ELISA (Fig. 4C) and were not able to block immunostaining of the cells with this antibody (Fig. 5B). No significant affinity of another antibody B1 (6C10) to the peptides was found in ELISA (data not shown). The residues 32-50 region is adapting α-helical conformation (Fig. 4B) in the three-dimensional structure of hTrpRS (Yang et al., 2003). Earlier the continuous antigenic determinant of mAb Am1 interacting with any eukaryotic TrpRS under reducing conditions was attributed to N-terminus (Favorova et al., 1989). However, according to sequence of this epitope (Zargarova et al., 1990) it apparently corresponds to Ileu/278–Ser/290 of hTrpRS and was wrongly attributed to N-terminus at that time. The full-length sequence of this protein was reported later (Garret et al., 1991; Frolova et al., 1991). Thus, the mAb B2 immunoreactive with the N-

terminal peptide in this study is directed to epitope, which had not been characterized previously. This epitope is located in the same region as the main HisRS autoepitope mapped within a helical amino-terminal region (Raben et al., 1994). This region contains WHEP-TRS (pfam00458) conserved domain common for TrpRS, HisRS, bifunctional GluRS/ProRS and GlyRS. The N-terminal extension presented only in mammalian but not bacterial TrpRS can be proteolytically deleted without effecting enzymatic activity (Lemaire et al., 1975).

3.3. Mapping of epitope of mAb B1 using phage-display library

Our data suggest that although mAb B1 is immunoreactive in Western blotting its epitope may be partially conformational. Specifically, the immunoreactivity of recombinant hTrpRS in Western blotting with this mAb is decreased following the protein boiling in the presence of β-mercaptoethanol (Fig. 2B). Second, in spite of the ability of this mAb to detect TrpRS in reducing Western blotting, the reaction was stronger under non-reducing conditions of ELISA and immunodot (data not shown). Hence, we employed a phage-display library technology for searching the conformational epitopes. This method is based on the production of large repertoires of random peptides expressed at N-terminus of the main coat protein (pVIII) of filamentous bacteriaphage fd. Through a cycle of selection and amplification, clones of antibody-bound phages can be identified and finally sequenced to reveal the amino acid sequence responsible for mAb binding. In such a manner the mAb B1 was used to screen the combinatorial phage display peptide libraries constructed at TAU where the filamentous phage contained the recombinant major coat pVIII protein displaying random 12 amino acid long peptides constrained by two cysteine residues. The 17 different positive phages were selected, cloned and confirmed by immunodot blot that they specifically bind the mAb B1 (data not shown). Then DNA of the individual phages was purified, sequenced and amino acid sequences of the corresponding peptides were deduced (Fig. 6A). Systemic analysis of the peptides did not reveal an obvious linear homology either among the phage sequences or with the original antigen. Therefore, localization of mAb B1 epitope was performed on the basis of computer algorithm (Enshell-Seijffers et al., 2003),

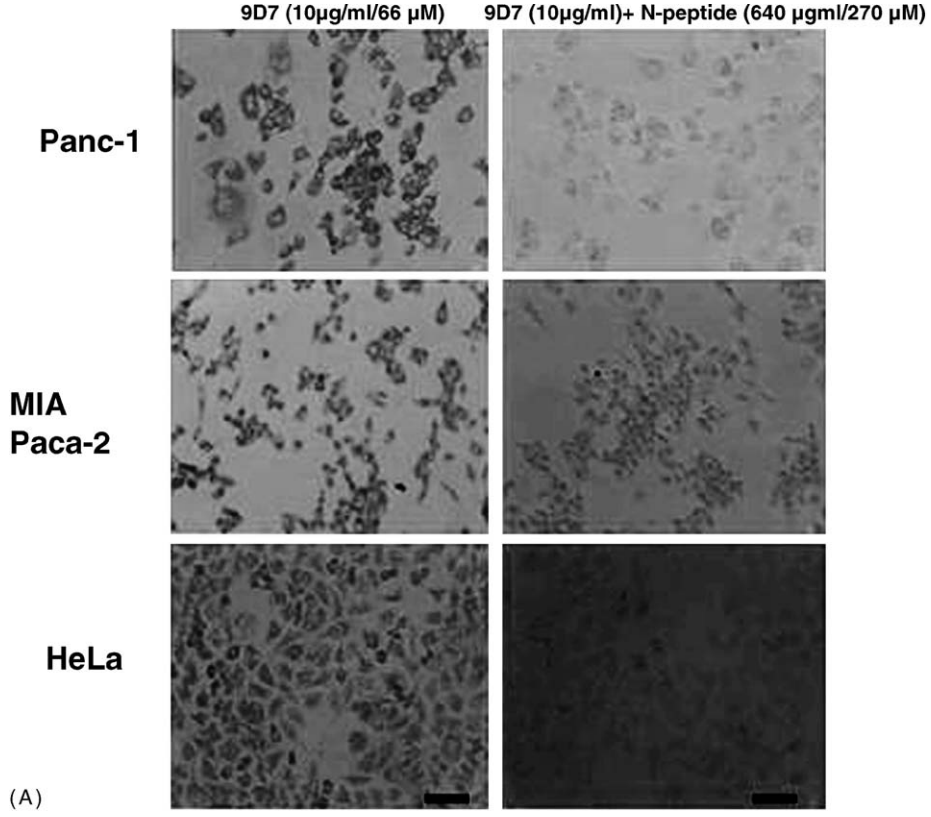

Fig. 5. Mapping of mAb B2 with synthetic peptides in immunocytochemistry of human cells. (A) Blocking of immunostaining of the methanol fixed 1420, 1469 and HeLa cells with N-peptide. All three cell lines are intensively immunostained with mAb B2 (left panels). The mAb B2 (9D7) depleted with a 4× molar excess of N-peptide failed to immunostain the cells (right panels). The cells were grown on the 24-wells plate (Corning). For depletion, the mAb B2 (25 μg/2.5 μl) was incubated with N-peptide (1.6 mg/2.5 ml) in the PBS buffer with 1 mg/ml BSA, 0.02% NaN_3, pH 7.2 for 75 min at room temperature. The mAb with and without N-peptide were spun 4 °C for 15 min at 12,000 rpm in the Beckman mini centrifuge. The cells were incubated with depleted and non-depleted mAb B2 overnight at 4 °C. The anti-mouse IgG peroxidase antibodies (Amersham)/1:400 were incubated for 30 min (400 μl/well) at room temperature. The peroxidase reaction was developed with AEC kit. Bars = 70 μm. (B) Immunostaining of the formaldehyde fixed human cells with 9D7 mAb (6 μg/ml/40 μM). The immunostaining was totally blocked by depletion with a molar excess of N-peptide but not M and C peptides (640 μg/ml/270 μM). The initial water solutions of each peptide were at 1.6 mg/ml. The peptides (1 ml) were incubated with 1.5 μl (15 μg) of mAb B2 (9D7) and 1 ml of the PBS buffer containing 1 mg/ml BSA, 0.1% NaN_3, pH 7.2 for 90 min at room temperature and overnight at 4 °C, then the mAb with and without peptides were spun. The cells were incubated with the mAbs overnight at 4 °C and treated as described above. Arrows show intensive immunostaining of TrpRS in mitotic cells (M) and immunostaining of filamentous-like structure (F). Bars = 35 μm.

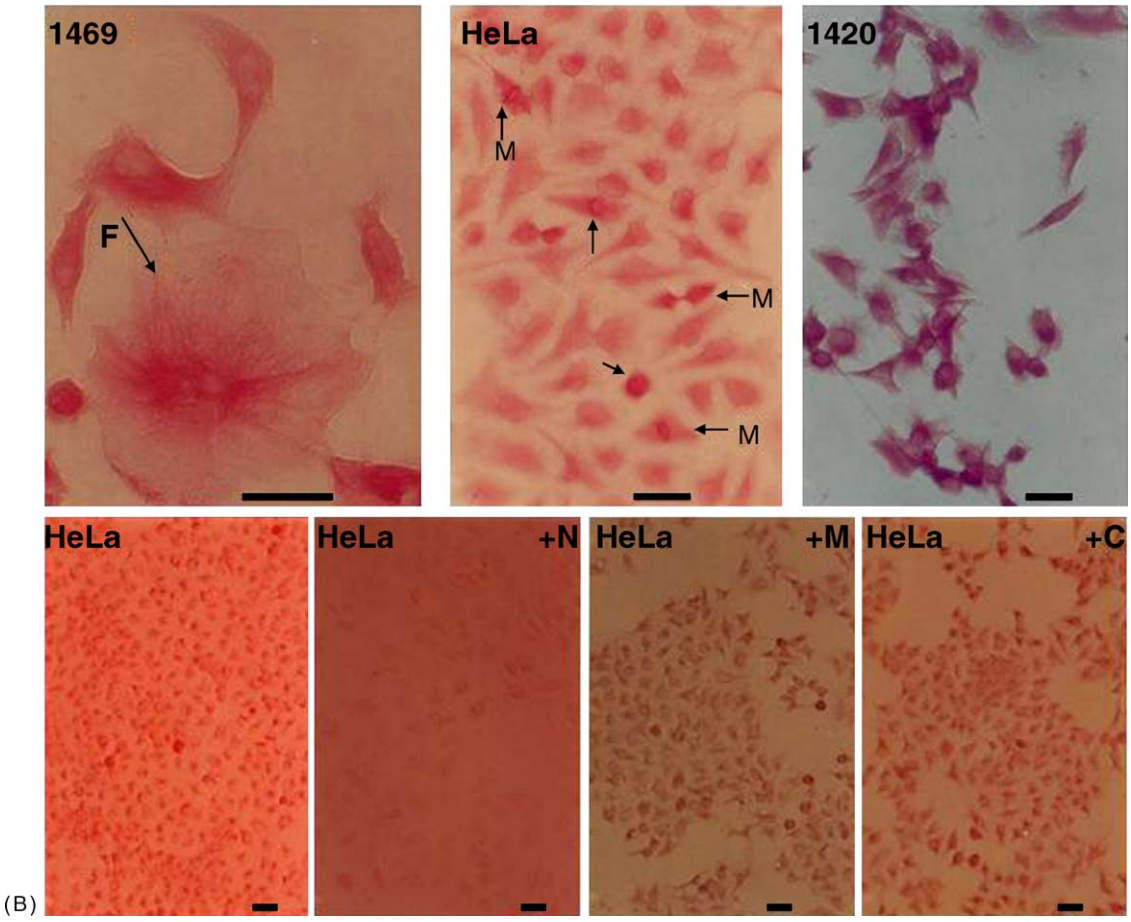

Fig. 5. (*Continued*).

which identifies the common denominators of the peptides and uses this information for localizing epitope onto the surface of the solved crystalline structure of hTrpRS (Yang et al., 2003). The experimental rationale is based on the assumption that the affinity-selected peptides derived from a vast collection of random peptides, due to their specific binding to the Ab of interest, must contain some structural or functional elements of the original epitope. The computer algorithm rationales, assumptions, and demonstration of the concept-feasibility are shortly outlined in the Methods and further discussed in detail (Enshell-Seijffers et al., 2003). Thus, the sequences of mAb 6C10 specific peptides (Fig. 6A) were analyzed by the computer algorithm. The predicted amino acid cluster is presented in Fig. 6B. This cluster resides at the carboxyl-terminus of TrpRS (Fig. 6C) within the residues Asp 409 to Met 425 where most of it acquires α-helical conformation.

To examine whether predicted epitope is immunoreactive with mAb 6C10 we constructed a bacteriophage vector fth1 containing insert coding 6C10 epitope (Fig. 6D). In order to evaluate whether or not the fth1 vector can produce 6C10 reactive peptide, a linker encoding the peptide DDDKLEQIRRDYTSGAA (a predicted 6C10 epitope with a single mutation Met425 → Ala) was inserted in-frame between the two *Sfi*I sites. The Ala425 was predicted by computer algorithm whereas Met425 presents in the reported TrpRS sequence. As demonstrated by dot blot analysis, the construct (fth1 6C10^{+}) can produce the phages that indeed bind the mAb 6C10 (Fig. 6E). The DNA from four independent highly positive clones was further analyzed. The DNA sequences from all four positive clones were identical to each other and to the predicted amino acids. It appeared that the mutation Met → Ala is not critical for the binding of the predicted epitope to mAb 6C10. The overlapping synthetic TrpRS-peptide corresponding to residues Glu414 to Val437 (C-peptide shown in Fig. 4A and B) exerted no immunoreactivity with the mAb 6C10 in ELISA. Thus, the residue/s within sequence 409/Asp-Asp-Asp-Lys/413 of the predicted epitope can be critical for binding of mAb 6C10 to TrpRS. The epitope mapping of this mAb identifies a region near the TrpRS C-terminus that remains accessible in oligomer (Fig. 2) and fibril alike (Fig. 7C), suggesting a model for the arrangement of subunits within TrpRS oligomers, protofibrils and fibrils. The 6C10 antibody can be useful for TrpRS monitoring, particularly the truncated carboxyl-TrpRS form possessing a potent anti-angiogenic activity (Tzima et al., 2005).

3.4. Disaggregation of TrpRS fibrils by antibody mAb B2

The earlier report describing high susceptibility of purified bTrpRS to aggregation (Tuzikov et al., 1991) and the present data demonstrating the presence of oligomers in the purified recom-

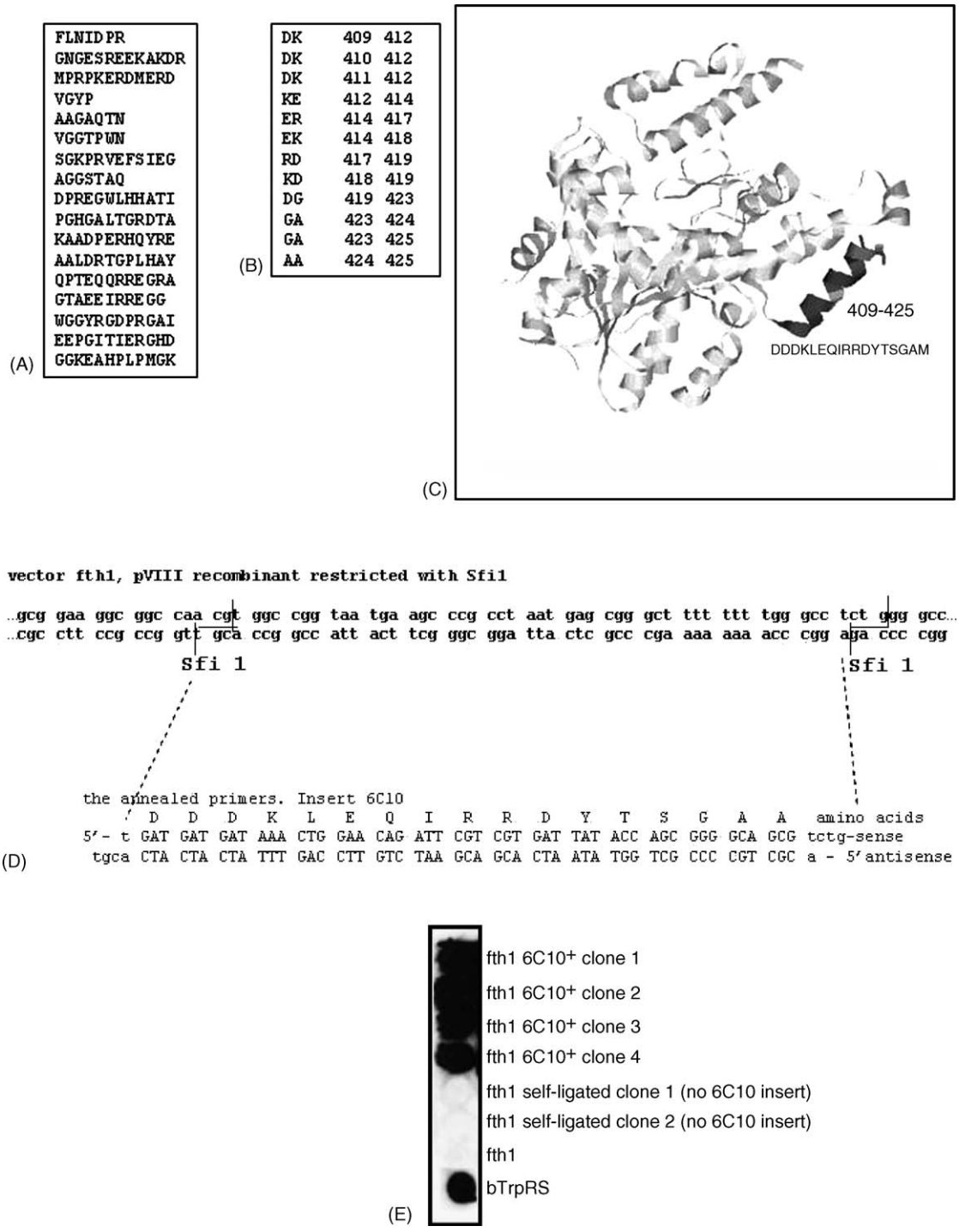

Fig. 6. Mapping of the mAb 6C10 (B1) epitope. (A) Affinity peptides selected by phage display library with the mAb 6C10. (B) Amino acid cluster found by computer algorithm. (C) RasMol presentation of hTrpRS three-dimensional model. (D) The 6C10 epitope fth1 phage construct. (E) Binding of mAb 6C10 to phages expressing 6C10 epitope. Equal amounts of phages 10^{10} to 10^{11}/50 μl were applied in duplicate to a nitrocellulose membrane and reacted with the mAb 6C10. The 6C10 epitope displaying phages fth1 showed strong signals. Phages fth1 were used as negative controls. The bTrpRS (0.8 μg/well) was used as a positive control. Note the 6C10^{+} construct did not bind the mAb 9D7.

binant hTrpRS and human neuroblastoma cells (Fig. 2) suggest the TrpRS aggregating ability. In addition, the TrpRS peptide 32-50 has amphipatic α-helical structure (Fig. 4B). Such structures are expected to aggregate in a water solution. One can see that within the protein it interacts by its hydrophobic side with another amphipatic α-helix 7-27. To examine the protein aggregation we stained the purified recombinant hTrpRS with Congo red and revealed the fibrils with a green apple birefringence (Fig. 7A). The Congo red staining enabled also to reveal fibrils formed by the N-peptide (1, 2.5, 5 and 10 mg/ml) and C-peptide (5 and 10 mg/ml) (Fig. 7B and C). The solutions of purified lyophilized mAb B1 or mAb B2 (6 mg/ml) were added to the

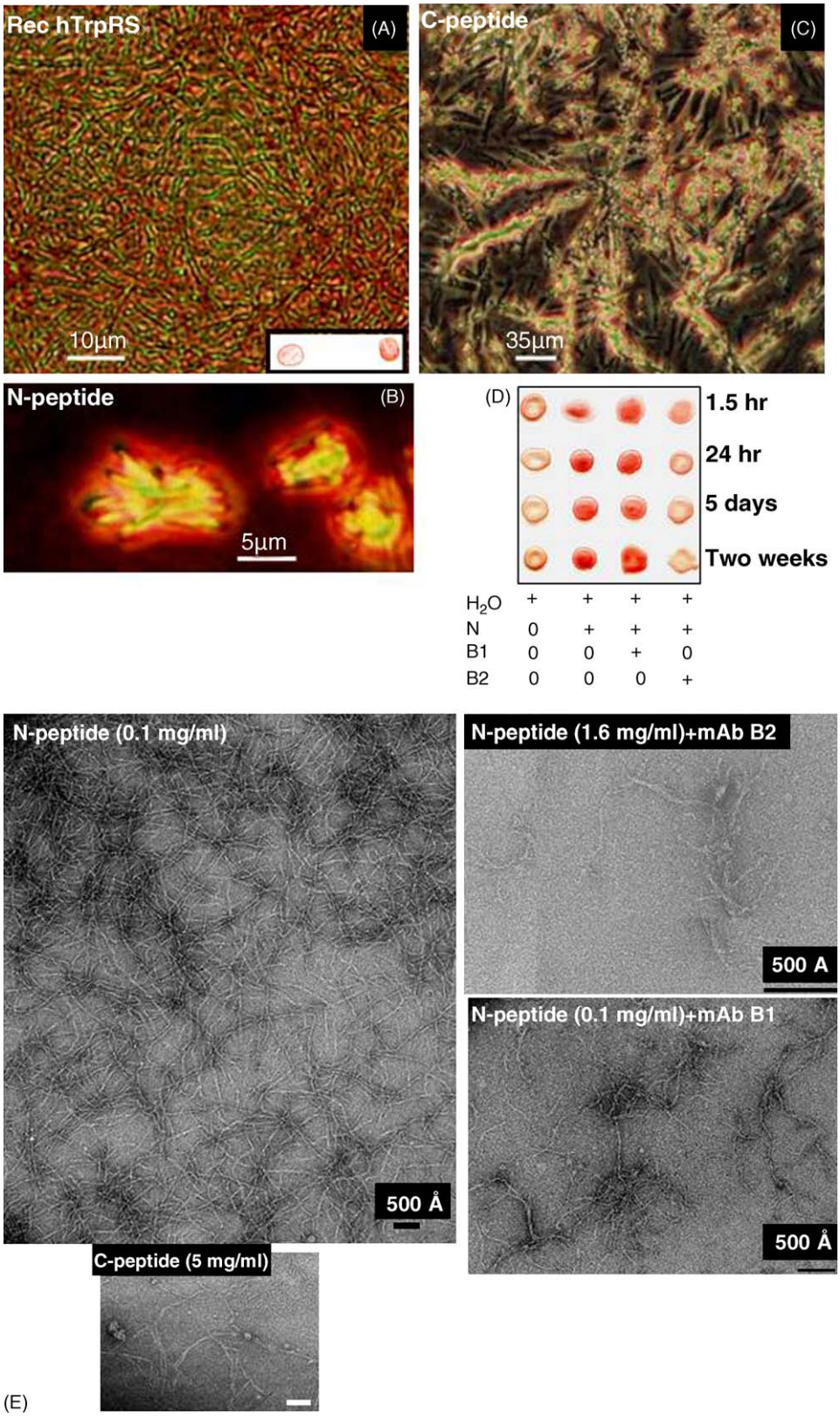

Fig. 7. TrpRS fibril formation and disaggregation by mAb B2. The panels A–D show the Congo red staining and birefringence and the panel E visualizes the electron microscopy images. The image A is a recombinant hTrpRS purified from the *E. coli* soluble fraction as described. The inset in the panel A shows the air dried drops of 2 μl of hTrpRS (8 mg/ml) stained with 4 μl of Congo red (right) and Congo red itself (left). The panels B and C show protofibrils formed by the N-peptide (2.5 mg/ml) and C-peptide (5 mg/ml), correspondingly. The panel D shows a glass slide with the N-peptide (N) before and after incubation with mAb B1 (B1) or mAb B2 (B2) for different periods. The panel E visualizes images of the N-peptide, C-peptide and disaggregation of the N-peptide fibrils by mAb B2, but not mAb

equal volume of peptides N, M, and C (10 mg/ml) and examined after Congo red staining (Fig. 7D). Following 4 days of incubation at a room temperature and 4 °C the samples were visualized under electron microscopy (Fig. 7E). The peptides alone were examined at the concentration 5 mg/ml and after dilution. The electron microscopy visualizes the intensive fibril formation by N-peptide (Fig. 7E). The C-peptide forms fewer less organized fibrils than N-peptide (Fig. 7E) whereas M-peptide forms no fibrils. The mAb B2 to the epitope located within N-peptide significantly decreased the density of the N-peptide fibrils (Fig. 7D and E). In contrast, the antibody B1 directed to the C-terminus has no effect on the fibril formation of the N-peptide (Fig. 7D and E). The mAb B2-mediated decrease in N-peptide fibril formation is correlated with a decrease in Congo red staining of this peptide observed after 90 min of the incubation with the mAb B2 at a room temperature (Fig. 7D). The data indicate that mAb B2 (9D7) bound to the N-peptide exerts disaggregating activity towards this peptide.

3.5. Cytotoxicity of TrpRS-derived peptides

Some fibrillogenic natural peptides, particularly β-amyloid (Zhang et al., 2002) and prion (Brown, 2000) are cytotoxic. We examined a potential effect of synthetic TrpRS-derived peptides on a cell viability and found that N-peptide is reproducibly cytotoxic for Mia PaCa-2 (1420) and Panc-1 (1469) cells whereas M and C peptides are not cytotoxic (data not shown). The N-peptide at 18 μM led to 40–50% cell death following 24–48 h of incubation. To compare, a cytotoxic prion peptide at 20 μM led to 50% cell death after 7 days of incubation (Brown, 2000). Thus, the N-peptide located within TrpRS N-terminal extension domain includes α-helical epitope of mAb 6C10, self-assembles in fibrils and has a significant cytotoxic effect.

3.6. Gel filtration of TrpRS and GluRS from SH-SY5Y human cells

To clarify whether TrpRS indeed presents in human cells as a high-molecular weight form we examined $tRNA^{trp}$ aminoacylation activity of SH-SY5Y cell extract fractionated by gel filtration on Sephacryl S400 (Fig. 8A). The aminoacylation activity of GluRS, a known component of the high-molecular weight ARS complex has been examined along with TrpRS activity. Both TrpRS and GuRS activities were eluted with a high-molecular weight standard Dextran blue as well as with lower molecular mass fractions. Thus, a portion of enzymatically active TrpRS presents in a high-molecular weight fraction of SH-SY5Y cells.

3.7. Immunodetection of co-immunoprecipitated TrpRS form

To examined whether the mAbs bind only free or also complexed form the presence of TrpRS was investigated following immunoprecipitation with mAbs to TrpRS or GluRS, the ∼160 kDa component of the ARS complex (Norcum, 1989). For immunoprecipitation we used the mAb F25 to the rabbit GluRS (Filonenko et al., 1991). No immunoreactivity corresponding to ∼160 kDa was detected in the extract of SH-SY5Y cells by immunoblotting with the F25. This is in agreement with the earlier studies that demonstrated no cross-reactivity of the 160-kDa hGluRS with the species-specific F25 (Filonenko et al., 1991; Wolfson, pers. commun.). Therefore, we used the rabbit kidney LCC-RK1 cells for immunoprecipitation with mAbs. Following immunoprecipitation the polypeptides of ∼160 kDa of GluRS (Fig. 8B, lane 1) or ∼55 kDa of TrpRS (Fig. 8B, lane 5) were revealed in immunoblotting with mAbs F25 and B1 (6C10), respectively. The ∼55 kDa TrpRS bands were also detected by Western blotting (Fig. 8B) with mAb B1 following immunoprecipitation with the mAb B1 (lane 3) and mAb B2 (lane 4) whereas no bands were detected by the control hybridoma medium (lane 2). Thus, at least a portion of cytoplasmic TrpRS is tightly associated with a cell fraction immunoprecipitated with mAb to GluRS. The TrpRS immunopreciptated with F25 (lane 5) binds to the mAb B1 in immunoblotting significantly stronger than the presumably free form immunoprecipitated with mAb B1 (lane 3) and mAb B2 (lane 4). The bTrpRS was shown to form a complex with glyceraldehyde-3-phosphate dehydrogenase (Filonenko et al., 1989). Earlier the co-localization of TrpRS with components of ARS complex in the RK1 cells was visualized by immuno-electron microscopy with the same mAb F25 (Ivanova et al., 1993; Popenko et al., 1994). This mAb was employed for immunoprecipitation of the ARS complex from the LCC-RK1 cells (Filonenko and Deutscher, 1994). For arginyl-tRNA synthetase the free and complexed forms are structurally distinct (Lazard and Mirande, 1993).

3.8. Immunohistochemistry

Several misfolding-mediated protein aggregation diseases such as Alzheimer's disease, Parkinson's disease and Huntington's disease have been modeled. Alzheimer disease (AD) is an age-dependent neurodegeneration of unknown etiology that is currently affected more than 4 million people in USA. AD is characterized by neurofibrillary tangles composed of paired helical filaments and extracellular senile plaques containing aggregated β-amyloid fibrils as well as non-amyloid components in brain. No effective treatment or biochemical tests for AD are currently available. The susceptibility of TrpRS and its

B1. The solutions of N-peptide (5 mg/ml) containing fibrils at a high density were diluted following incubation with mAbs (3 mg/ml). The peptide concentrations shown on the images were used for observation in electron microscope. Note the dense fibrils of the N-peptide are visible at the concentration 0.1 mg/ml whereas only few N-peptide fibrils are detectable at a concentration of 1.6 mg/ml following incubation with mAb B2. Bars = 500 Å. (For interpretation of the references to colour in this figure legend, the reader is referred to the web version of the article).

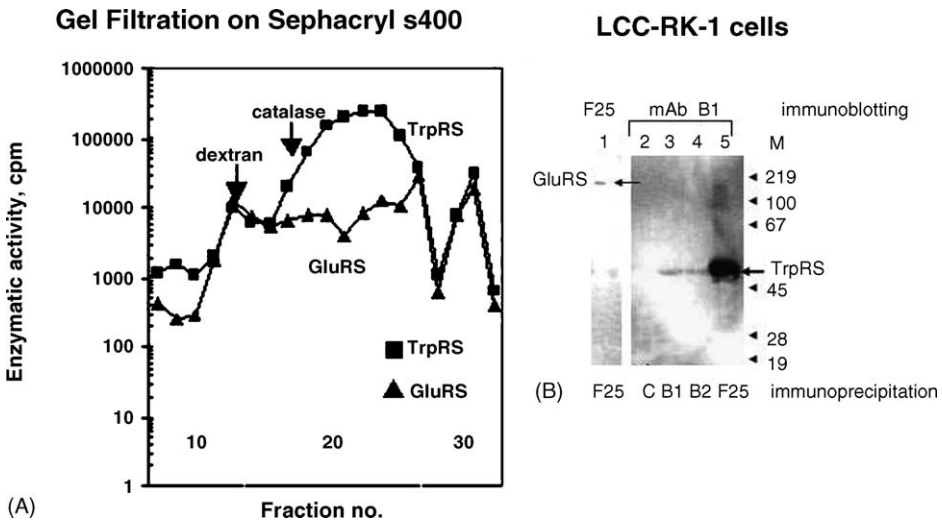

Fig. 8. TrpRS coelution and coimmunoprecipitation. (A) Aminoacylation of $tRNA^{trp}$ and $tRNA^{glu}$ following gel filtration of SH-SY5Y cytoplasmic extract on Sephacryl S400 column. Note GluRS and TrpRS are coeluted with a high molecular weight fraction and Dextran Blue in the void volume of the column. (B) Western immunoblotting with mAb F25 to GluRS (lane 1) and mAb B1 to TrpRS (lanes 2–5) followed the immunoprecipitation of the LCC-RK1 cells. The cell extracts were immunoprecipitated with mAb F25 (F25, lanes 1 and 5), control hybridoma medium (C, lane 2), mAb B1 (lane 3) and mAb B2 (lane 4) supernatants. Note TrpRS is coimmunoprecipitated with GluRS (compare lanes 1 and 5) where the ~50 kDa TrpRS polypeptide is detected by blot with mAb B1 (lane 5) following immunoprecipitation with anti-GluRS mAb F25 and a ~160 kDa polypeptide (lane 1), corresponding to molecular mass of GluRS was detected in immunoblotting with mAb F25. M shows positions of molecular weight markers in kDa.

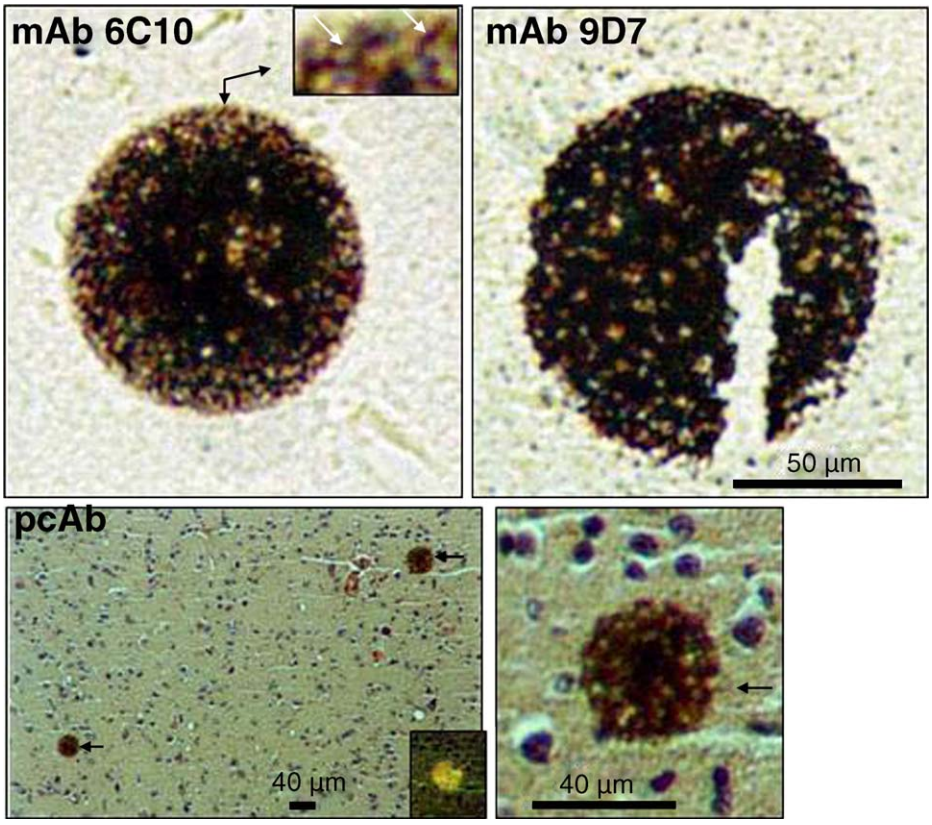

Fig. 9. TrpRS-positive pathology in brain of Alzheimer's disease patients. The brain areas are superior frontal gyrus (upper left image), superior parietal lobule (upper right image) and hippocampus (low panels). The anti-TrpRS undiluted 6C10 and 9D7 hybridoma supernatants (upper images) and polyclonal anti-TrpRS sera (pcAb, 1:100) were used for immunostaining. The inset in upper left panel shows a high-power magnification of TrpRS-positive twisted filamentous-like pathology. The peroxiadse reaction was developed with diaminobenzidine. The counterstaining with hematoxylin/Congo red following immunostaining with anti-TrpRS was conducted for the lower and not the upper images. The inset in the low panel shows birefringence of TrpRS-positive formation (arrow) after Congo red staining. The right low image is a higher magnification of the characteristic TrpRS-pathology visualized on the left low panel. The control staining with the only peroxidase antibodies was negative.

Table 1
TrpRS epitopes in different species

Species	Sequence	References	Reactivity
Epitope 6C10			
Bovine	DDDKLEQIRRDYTSGAM	Garret et al. (1991)	+
Human	DDDKLEQIRKDYTSGAM	Frolova et al. (1991)	+
Rabbit	DDDKLEQIRKDYSSGAM	Frolova et al. (1993)	+
E. coli	QSIPELEKQFE---GKM	Hall et al. (1982)	−
Mouse	DDDRLEQIRKDYTSGAM	Pajot et al. (1994)	N/D
Dros.	DDAKLEEVRVAYSKGEM	Seshaiah and Andrew (1999)	N/D
Epitope 9D7			
Bovine	AKDEIDSAVKMLLSLKTSY	Garret et al. (1991)	+
Human	SKDEIDSAVKMLVSLKMSY	Frolova et al. (1991)	+
Rabbit	PKEEIDSAVKMLLSLKTSY	Frolova et al. (1993)	+
Mouse	PKDEIDSAVKMLLSLKMSY	Pajot et al. (1994)	N/D
Dros.	MADTKETVVEGVEALTLNG	Seshaiah and Andrew (1999)	N/D

(+) Positive reaction; (−) negative reaction; (N/D) non-examined; amino acid changes are underlined.

fragments to aggregation encouraged us to examine the presence of TrpRS in AD brain using monoclonal and polyclonal antibodies to TrpRS. Immunohistochemical analysis of brain sections with both 6C10 and 9D7 mAbs revealed prominent staining of extracellular plaque-like compact formations (Fig. 9) in hippocampus, superior frontal gyrus and superior parietal lobule of the eight examined AD patients but not of the five control brains or after staining with the mAbs blocked by recombinant hTrpRS. The apparently fibril-like material is visualized on the periphery of the round-shape plaques by immunostaining (Fig. 9, upper left image). The TrpRS-positive formations with similar morphology were also detected with polyclonal sera (Fig. 9, low image). Some $TrpRS^{+}$-plaques were studied after double-staining with Congo red. The Congo-red positive $TrpRS^{+}$-plaques express birefringence (Fig. 9, low panel, inset). The TrpRS-positive plaques up to 100 μm in diameter were detected in amount one to three or none per one brain section with the approximate to oval size of ∼15 mm × 20 mm. The evidence from tissue culture, in vivo models, and AD brain studies indicate that inflammation in AD is mediated by the production of pro-inflammatory molecules, leading to microglial activation and neuronal damage (Ho et al., 2005). The link of TrpRS to inflammation (Ivakhno and Kornelyuk, 2004) may at least partially explain the appearance of TrpRS manifestaions in AD brain. In addition, it was shown recently that TrpRS is upregulated in the epidermis of elderly individuals (Gromov et al., 2003). The aggregation with fibril formation of TrpRS and its peptides shown here may lead to formation of the TrpRS containing aggregates discovered in AD brain by using new developed mAbs.

3.9. Analysis of species-specific cross-reactivity of mAbs 6C10 and 9D7

A single species-specific (bovine/human) conservative change Arg/Lys is located at the positions $bTrpRS/Arg^{422} \rightarrow hTrpRS/Lys^{418}$ (Garret et al., 1991; Frolova et al., 1991) in the epitope 6C10 (Table 1). Because the bTrpRS reacts better than hTrpRS with the mAb 6C10 in the Western blotting we suggest that Arg/Lys substitution may be essential, but not critical for immunoreactivity of this epitope. The sequences, which may correspond to the 6C10 epitope are near identical in rabbit (Frolova et al., 1993) and human TrpRS (Frolova et al., 1991) and are very different from *E. coli* TrpRS (Hall et al., 1982). This may explain the cross-reactivity of mAb 6C10 with rabbit TrpRS and absence of reactivity with *E. coli* TrpRS in Western blotting. A single conservative change Thr/Ser in the rabbit TrpRS may indicate that Thr/Ser substitution is not critical for immunoreactivity of this epitope. The 6C10 epitope-like region possesses two conservative changes Arg/Lys and Lys/Arg in mouse TrpRS (Pajot et al., 1994) and many changes in this region of *Drosophila* TrpRS (Seshaiah and Andrew, 1999). The region of hTrpRS that corresponds to epitope 9D7 contains three changes and rabbit TrpRS contains two changes in comparison with a bovine counterpart (Table 1). These changes seem not critical since immunoreactivity of human and rabbit TrpRS with mAb 9D7 is preserved. The 9D7 epitope-like domain presents in mouse TrpRS, has a low homology with the *Drosophila* TrpRS and absent in the bacterial TrpRS. No domains with a homology to both 6C10 and 9D7 epitopes are present in the mitochondrial hTrpRS (Jorgensen et al., 2000). Thus, both 6C10 and 9D7 epitopes seem conservative among cytoplasmic TrpRS of mammals and distinctive from mitochondria, bacteria, and insect. Therefore, mAbs 6C10 and 9D7 could be used for detection of epitopes intrinsic to mammals discriminating epitopes associated with bacterial and insect invasion.

Acknowledgements

This work was supported in parts by Fellowship from the Howard Hughes Medical Institute (O.S.), Grants from the Israel Ministries of Health and Science (E.L.P.), Fellowship from the Gileadi Program of the Israel Inter-University Commission (E.L.P.) and Grant from the Israel Science Foundation (G.D.). We thank Dr. Valery Filonenko for providing mAb F25, Dr. Niko Grigorieff for help with electron microscopy and Dr. Olga Volpert for support. The mAbs 6C10 and 9D7 used in this study were produced at the Expert BioMed, Inc.

References

Bandyopadhyay, A.K., Deutscher, M.P., 1971. Complex of aminoacyl-tRNA synthetases. J. Mol. Biol. 60, 113–122.

Beresten, S.F., Zargarova, T.A., Favorova, O.O., Rubikaite, B.I., Ryazanov, A.G., Kisselev, L.L., 1989. Molecular and cellular studies of tryptophanyl-tRNA synthetase using monoclonal antibodies. Evaluation of a common antigenic determinant in eukaryotic, prokaryotic and archaebacterial enzymes which maps outside the catalytic domain. Eur. J. Biochem. 184, 575–581.

Biedler, J., Helson, L., Spengler, B.A., 1973. Morphology and growth, tumorigenicity, and cytogenetics of human neuroblastoma cells in continuous culture. Cancer Res. 33, 2643–2652.

Bolgarin, R.N., Rodnin, N.V., Sidorik, L.L., 1998. Autoantibodies to tryptophanyl-tRNA-synthetase in systemic autoimmune diseases. Mol. Biol. (Mosk.) 32, 745–749.

Brown, D.R., 2000. Altered toxicity of the prion protein peptide PrP106–126 carrying the $Ala^{117} \rightarrow Val$ mutation. Biochem. J. 346, 785–791.

Du, L.L., Novick, P., 2001. Purification and properties of a GTPase-activating protein for yeast Rab GTPases. Methods Enzymol. 329, 91–99.

Enshell-Seijffers, D., Smelyanski, L., Gershoni, J.M., 2001. The rational design of a 'type 88' genetically stable peptide display vector in the filamentous bacteriophage fd. Nucl. Acids Res. 29, E50-0.

Enshell-Siejffers, D., Gershoni, J.M., 2002. Phage-display selection and analysis of Ab-binding epitopes. In: Coligan, A.M.K., Margulies, D.H., Strober, W. (Eds.), Current Protocols in Immunology. John Wiley & Sons, New York.

Enshell-Seijffers, D., Denisov, D., Groisman, B., Smelyanski, L., Meyuhas, R., Gross, G., Denisova, G., Gershoni, J.M., 2003. The mapping and reconstitution of a conformational discontinuous b-cell epitope of HIV-1. J. Mol. Biol. 334, 87–101.

Favorova, O.O., Zargarova, T.A., Rukosuyev, V.S., Beresten, S.F., Kisselev, L.L., 1989. Molecular and cellular studies of tryptophanyl-tRNA synthetases using monoclonal antibodies. Remarkable variations in the content of tryptophanyl-tRNA synthetase in the pancreas of different mammals. Eur. J. Biochem. 184, 583–588.

Filonenko, V.V., Beresten, S.F., Rubikaite, B.I., Kisselev, L.L., 1989. Bovine tryptophanyl-tRNA synthetase and glyceraldehyde-3-phosphate dehydrogenase form a complex. Biochem. Biophys. Res. Commun. 161, 481–488.

Filonenko, V.V., Wolfson, A.D., Wartanyan, O.A., Beresten, S.F., 1991. Monoclonal antibodies to the components of the high-molecular-mass aminoacyl-tRNA synthetase complex. Biomed. Sci. 2, 289–292.

Filonenko, V.V., Deutscher, M.P., 1994. Evidence for similar structural organization of the multienzyme aminoacyl-tRNA synthetase complex in vivo and in vitro. J. Biol. Chem. 269, 17375–17378.

Fodinger, M., Fritsche-Polanz, R., Buchmayer, H., Skoupy, S., Sengoelge, G., Horl, W.H., Sunder-Plassmann, G., 2000. Erythropoietin-inducible immediate-early genes in human vascular endothelial cells. J. Invest. Med. 48, 137–149.

Frolova, L.Yu., Dalphin, M.E., Justesen, J., Powell, R.J., Drugeon, G., McCaughan, K.K., Kisselev, L.L., Tate, W.P., Haenni, A.L., 1993. Mammalian polypeptide chain release factor and tryptophanyl-tRNA synthetase are distinct proteins. EMBO J. 12, 4013–4019.

Frolova, L.Yu., Sudomoina, M.A., Grigorieva, A.Yu., Zinovieva, O.L., Kisselev, L.L., 1991. Cloning and nucleotide sequence of the structural gene encoding for human tryptophanyl-tRNA synthetase. Gene 109, 291–296.

Galfre, G., Milstein, C., 1981. Preparation of monoclonal antibodies: strategies and procedures. Methods Enzymol. 73 (Pt B), 3–46.

Garret, M., Pajot, B., Trezeguet, V., Labouesse, J., Merle, M., Gandar, J.C., Benedetto, J.P., Sallafranque, M.L., Alterio, J., Gueguen, M., Sarger, C., Labouesse, B., Bonnet, J., 1991. A mammalian tryptophanyl-tRNA synthetase shows little homology to prokaryotic synthetases but near identity with mammalian peptide chain release factor. Biochemistry 30, 7809–7817.

Gromov, P., Skovgaard, G.L., Palsdottir, H., Gromova, I., Ostergaard, M., Celis, J.E., 2003. Protein profiling of the human epidermis from the elderly reveals up-regulation of a signature of interferon-{gamma}-induced polypeptides that includes manganese-superoxide dismutase and the p85{beta} subunit of phosphatidylinositol 3-kinase. Mol. Cell. Proteomics 2, 70–84.

Gros, C., Le Maire, G., Van Rapenbusch, R., Labouesse, B., 1972. The subunit structure of tryptophanyl transfer ribonucleic acid synthetase from beef pancreas. J. Biol. Chem. 247, 2931–2943.

Hall, C.V., vanCleemput, M., Muench, K.H., Yanofsky, C., 1982. The nucleotide sequence of the structural gene for *Escherichia coli* tryptophanyl-tRNA synthetase. J. Biol. Chem. 257, 6132–6136.

Harlow, E., Lane, D., 1988. Storing and purifying antibodies. In: Antibodies: A Laboratory Manual. Cold Spring Harbor Laboratory Press, Cold Spring Harbor, NY, pp. 283–319.

Ho, G.J., Drego, R., Hakimian, E., Masliah, E., 2005. Mechanisms of cell signaling and inflammation in Alzheimer's disease. Curr. Drug Targets Inflamm. Allergy 4, 247–256.

Hull, R.N., Dwyer, A.C., Cherry, W.R., Tritch, O.J., 1965. Development and characteristics of the rabbit kidney cell strain, LLC-RK1. Proc. Soc. Exp. Biol. Med. 118, 1054–1059.

Iborra, F., Labouesse, B., Labouesse, J., 1975. Structure–activity relationships in tryptophanyl transfer ribonucleic acid synthetase from beef pancreas. Influence of alkylation of the sulfhydryl groups on the dimer-monomer equilibrium. J. Biol. Chem. 250, 6659–6665.

Ivakhno, S.S., Kornelyuk, A.I., 2004. Cytokine-like activities of some aminoacyl-tRNA synthetases and auxiliary p43 cofactor of aminoacylation reaction and their role in oncogenesis. Exp. Oncol. 26, 250–255.

Ivanova, Iu. L., Cherni, N.E., Popenko, V.I., Filonenko, V.V., Vartanian, O.G., 1993. Comparative study of localization of tryptophanyl-tRNA-synthetase and components of high molecular weight aminoacyl-tRNA-synthetase complex in animal cells. Mol. Biol. (Mosk.) 27, 666–684.

Jorgensen, R., Sogaard, T.M., Rossing, A.B., Martensen, P.M., Justesen, J., 2000. Identification and characterization of human mitochondrial tryptophanyl-tRNA synthetase. J. Biol. Chem. 275, 16820–16826.

Krause, S.W., Rehli, M., Kreutz, M., Schwarzfischer, L., Paulauskis, J.D., Andreesen, R., 1996. Differential screening identifies genetic markers of monocyte to macrophage maturation. J. Leukoc. Biol. 60, 540–545.

Lazard, M., Mirande, M., 1993. Cloning and analysis of a cDNA encoding mammalian arginyl-tRNA synthetase, a component of the multisynthetase complex with a hydrophobic N-terminal extension. Gene 132, 237–245.

Lefevre, T., Arseneault, K., Pezolet, M., 2004. Study of protein aggregation using two-dimensional correlation infrared spectroscopy and spectral simulations. Biopolymers 73, 705–715.

Lemaire, G., Gros, C., Epely, S., Kaminski, M., Labouesse, B., 1975. Multiple forms of tryptophanyl-tRNA synthetase from beef pancreas. Eur. J. Biochem. 51, 237–252.

Lieber, M., Mazzetta, J., Nelson-Rees, W., Kaplan, M., Todaro, G., 1975. Establishment of a continuous tumor-cell line (panc-1) from a human carcinoma of the exocrine pancreas. Int. J. Cancer 15, 741–747.

Lipscomb, M.S., Lee, M.-L., Muench, K.H., 1976. Human tryptophanyl transfer ribonucleic acid synthetase. Composition, function of thiol groups, and structure of thiol peptides. J. Biol. Chem. 251, 3261–3268.

Matsunaga, T., Ishida, T., Takekawa, M., Nishimura, S., Adachi, M., Imai, K., 2002. Analysis of gene expression during maturation of immature dendritic cells derived from peripheral blood monocytes. Scand. J. Immunol. 56, 593–601.

Miller, F.W., Waite, K.A., Biswas, T., Plotz, P.H., 1990. The role of an autoantigen, histidyl-tRNA synthetase, in the induction and maintenance of autoimmunity. Proc. Natl. Acad. Sci. U.S.A. 87, 9933–9937.

Muller, P.Y., Janovjak, H., Miserez, A.R., Dobbie, Z., 2002. Processing of gene expression data generated by quantitative real-time RT-PCR. Biotechniques 32, 1372–1379.

Norcum, M.T., 1989. Isolation and electron microscopic characterization of the high molecular mass aminoacyl-tRNA synthetase complex from murine erthroleukemia cells. J. Biol. Chem. 284, 15043–15061.

Ohtani, M., Kobayashi, Y., Watanabe, N., 2004. Gene expression in the elicitation phase of guinea pig DTH and CHS reactions. Cytokine 25, 246–253.

Pajot, B., Sarger, C., Bonnet, J., Garret, M., 1994. An alternative splicing modifies the C-terminal end of tryptophanyl-tRNA synthetase in murine embryonic stem cells. J. Mol. Biol. 242, 599–603.

Paley, E.L., Baranov, V.N., Alexandrova, N.M., Kisselev, L.L., 1991. Tryptophanyl-tRNA synthetase in cell lines resistant to tryptophan analogs. Exp. Cell Res. 195, 66–78.

Paley, E.L., Alexandrova, N., Smelansky, L., 1995. Tryptophanyl-tRNA synthetase as a human antigen. Immunol. Lett. 48, 201–207.

Paley, E.L., 1997. A mammalian tryptophanyl-tRNA synthetase is associated with protein kinase activity. Eur. J. Biochem. 244, 780–788.

Paley, E.L., 1999. Tryptamine-mediated stabilization of tryptophanyl-tRNA synthetase in human cervical carcinoma cell line. Cancer Lett. 137, 1–7.

Penneyes, N.S., Muench, K.H., 1974. Human placental transfer ribonucleic acid synthetase. Purification and subunit structure. Biochemistry 13, 560–565.

Popenko, V.I., Ivanova, J.L., Cherny, N.E., Filonenko, V.V., Beresten, S.F., Wolfson, A.D., Kisselev, L.L., 1994. Compartmentalization of certain components of the protein synthesis apparatus in mammalian cells. Eur. J. Cell Biol. 65, 60–69.

Raben, N., Nichols, R., Dohlman, J., McPhien, P., Sridharll, V., Hydell, C., Richard Leff, R., Plotz, P., 1994. A motif in human histidyl-tRNA synthetase which is shared among several aminoacyl-tRNA synthetases is a coiled-coil that is essential for enzymatic activity and contains the major autoantigenic epitope. J. Biol. Chem. 269, 24277–24283.

Ramsden, D.A., Chen, J., Miller, F.W., Misener, V., Bernstein, R.M., Siminovitch, K.A., Tsui, F.W., 1989. Epitope mapping of the cloned human autoantigen, histidyl-tRNA synthetase. Analysis of the myositis-associated anti-Jo-1 autoimmune response. J. Immunol. 143, 2267–2272.

Rubin, B.Y., Anderson, S.L., Xing, L., Powell, R., Tate, W.P., 1991. Interferon induces tryptophanyl-tRNA synthetase expression in human fibroblasts. J. Biol. Chem. 266, 24245–24248.

Salvucci, O., Basik, M., Yao, L., Bianchi, R., Tosato, G., 2004. Evidence for the involvement of SDF-1 and CXCR4 in the disruption of endothelial cell-branching morphogenesis and angiogenesis by TNF-alpha and IFN-gamma. J. Leukoc. Biol. 76, 217–226.

Scheinker, V.S., Beresten, S.F., Mazo, A.M., Ambartsumyan, N.S., Rokhlin, O.V., Favorova, O.O., Kisselev, L.L., 1979. Immunochemical studies of beef pancreas tryptophanyl-tRNA synthetase and its fragments. Determination of the number of antigenic determinants and a comparison with tryptophanyl-tRNA synthetases from other sources and with reverse transcriptase from avian myeloblastosis virus. Eur. J. Biochem. 97, 529–540.

Seshaiah, P., Andrew, 1999. D.J. WRS-85D: a tryptophanyl-tRNA synthetase expressed to high levels in the developing Drosophila salivary gland. Mol. Biol. Cell 10, 1595–1608.

Sokolova, O., Accardi, A., Gutierrez, D., Lau, A., Rigney, M., Grigorieff, N., 2003. Conformational changes in the C terminus of Shaker K+ channel bound to the rat Kvbeta2-subunit. Proc. Natl. Acad. Sci. U.S.A. 100, 12607–12612.

Targoff, I.N., 2002. Idiopathic inflammatory myopathy: autoantibody update. Curr. Rheumatol. Rep. 5, 434–441.

Tuzikov, F.V., Tuzikova, N.A., Vavilin, V.I., Zinov'ev, V.V., Malygin, E.G., Favorova, O.O., Zargarova, T.A., Sudomoina, M.A., Kisselev, L.L., 1991. Aggregation of tryptophanyl-tRNA synthetase depending on temperature. Study by a low-angle scatter X-ray method. Mol. Biol. (Mosk.) 25, 740–751.

Tzima, E., Reader, J.S., Irani-Tehrani, M., Ewalt, K.L., Schwartz, M., Schimmel, P., 2005. VE-cadherin links tRNA synthetase cytokine to anti-angiogenic function. J. Biol. Chem. 280, 2405–2408.

Vartanian, O.A., 1991. Detection of autoantibodies against phenylalanyl-, tyrosyl-, and tryptophanyl-tRNA-synthetase and anti-idiotypic antibodies to it in serum from patients with autoimmune diseases. Mol. Biol. (Mosk.) 25, 1033–1039.

Yang, X.-L., Otero, F.J., Skene, R.J., McRee, D.E., Schimmel, P., Ribas de Pouplana, L., 2003. Crystal structures that suggest late development of genetic code components for differentiating aromatic side chains. Proc. Natl. Acad. Sci. 100, 15376–15380.

Yunis, A.A., Arimura, G.K., Russin, D.J., 1977. Human pancreatic carcinoma (MIA PaCa-2) in continuous culture: sensitivity to asparaginase. Int. J. Cancer 19, 218–235.

Zargarova, T.A., Zargarov, A.A., Bolotina, I.A., Beresten', S.F., Favorova, O.O., 1990. A peptide, containing the universal antigenic determinant of tryptophanyl-tRNA-synthetase. Bioorg. Khim. 16, 1259–1267.

Zhang, Y., McLaughlin, R., Goodyer, C., LeBlanc, A., 2002. Selective cytotoxicity of intracellular amyloid peptide 1-42 through p53 and Bax in cultured primary human neurons. J. Cell Biol. 156, 519–529.